J|A|C|S
ARTICLES
Published on Web 12/06/2006

Influence of Single-Walled Carbon Nanotubes Induced Crystallinity Enhancement and Morphology Change on Polymer Photovoltaic Devices

Jianxin Geng and Tingying Zeng*

Contribution from the Laboratory of Nanostructures, Department of Chemistry, Western Kentucky University, 1906 College Heights Blvd 11079, Bowling Green, Kentucky 42101-1079

Received July 14, 2006; E-mail: tingying.zeng@wku.edu

Abstract: Single-walled carbon nanotubes (SWNTs) were determined to have significant interaction with poly(3-hexylthiophene) (P3HT), which is helpful to form continuous active film with interpenetrating structure and improve the crystallinity of the resultant film for SWNTs/P3HT composite. Photovoltaic devices based on an active film with relatively higher crystallinity display much enhanced performance. The work function of carbon nanotubes modulated by electron transferring from P3HT to SWNTs is proposed to explain the high open-circuit voltage (V_{OC}) obtained from the photovoltaic devices based on the SWNTs/P3HT system.

Introduction

As a renewable and alternative source for conversion to electric power, solar energy is a potential choice to handle the crisis of exhausted fossil energy. Polymeric photovoltaic devices have attracted great interest over the past 20 years due to low fabrication costs, ease of processing, and mechanical flexibility.[1] In polymeric photovoltaic devices, a donor−acceptor regime is required to enhance the efficiency of exciton generation, dissociation, and charge transportation. As acceptors, fullerene,[2] nanoparticle,[3] carbon nanotubes,[4,5] and conjugated polymer with higher electron affinity[6] were selected to hybrid with semiconducting polymer, polythiophene or poly(*p*-phenylene vinylene) (PPV), serving as donor and transportation media for holes.

Since the discovery of photoinduced charge transfer between organic conjugated polymers (as donor) and nanotubes (as acceptor), both multiwalled carbon nanotubes (MWNTs)[7] and single-walled carbon tubes (SWNTs)[4,5] have been used to fabricate photovoltaic devices in combination with PPV and polythiophene. Electron−hole pairs, excitons, are generated at the interface of polymers and carbon nanotubes upon illumination. Having a larger electron affinity than the polymer, carbon nanotubes serve as electron traps. Charge dissociation occurs with electrons going to carbon nanotubes and holes going to polymers. The first report of a polymer/SWNTs photovoltaic device was in 2002, utilizing arc discharged SWNTs/poly(3-octylthiophene) (P3OT) composite.[4] An open-circuit voltage (V_{OC}) as high as 0.75 V was obtained for a 1% doped SWNTs/P3OT composite active layer. However, the maximum V_{OC} of the reported case should be about 0.4 V based on the metal−insulator−metal (MIM) model. The work function is 4.3 eV for Al and 4.7 eV for indium−tin oxide (ITO).[8] Therefore, the MIM model may not be applicable to the SWNTs/P3OT system since the obtained V_{OC} is much higher than that theoretically anticipated. In order to interpret the mechanism of this high open-circuit voltage, researchers proposed an internal SWNTs/P3OT junction between the highest occupied molecular orbit (HOMO) of P3OT and the work function of SWNTs based on ohmic contacts between SWNTs and metal electrode.[4b]

From the viewpoint of the relationship between structure and performance, a nanocrystalline structure with high crystallinity is pursued so that a relatively higher transportation speed for holes is obtained via interchain transport of charge carriers.[9] Interestingly, the performance of a photovoltaic device based on P3HT is strongly dependent on the processing condition, especially enhancement of the crystallinity of the active layer by thermal treatment. In J. Loos's experiment based on [6,6]-phenyl C61 butyric acid methyl ester (PCBM) and P3HT, thermal treatment was applied to the final devices and the

(1) (a) Halls, J. J. M.; Walsh, C. A.; Greenham, N. C.; Marseglia, E. A.; Friend, R. H.; Moratti, S. C.; Holmes, A. B. *Nature* **1995**, *376*, 498. (b) Granström, M.; Petritsch, K.; Arias, A. C.; Lux, A.; Andersson, M. R.; Friend, R. H. *Nature* **1998**, *395*, 275.
(2) (a) Yu, G.; Gao, J.; Hummelen, J. C.; Wudl, F.; Heeger, A. J. *Science* **1995**, *270*, 1789. (b) Campos, L. M.; Tontcheva, A.; Günes, S.; Sonmez, G.; Neugebauer, H.; Sariciftci, N. S.; Wudl, F. *Chem. Mater.* **2005**, *17*, 4031.
(3) (a) Huynh, W. U.; Dittmer, J. J.; Alivisatos, A. P. *Science* **2002**, *295*, 2425. (b) Liu, J.; Tanaka, T.; Sivula, K.; Alivisatos, A. P.; Fréchet, J. M. J. *J. Am. Chem. Soc.* **2004**, *126*, 6550.
(4) (a) Kymakis, E.; Amaratunga, G. A. J. *Appl. Phys. Lett.* **2002**, *80*, 112. (b) Kymakis, E.; Alexandrou, I.; Amaratunga, G. A. J. *J. Appl. Phys.* **2003**, *93*, 1764.
(5) (a) Landi, B. J.; Raffaelle, R. P.; Castro, S. L.; Bailey, S. G. *Prog. Photovolt. Res. Appl.* **2005**, *13*, 165. (b) Landia, B. J.; Castrob, S. L.; Rufa, H. J.; Evansa, C. M.; Baileyc, S. G.; Raffaelle, R. P. *Sol. Energy Mater. Sol. Cell* **2005**, *87*, 733.
(6) (a) Alam, M. M.; Jenekhe, S. A. *Chem. Mater.* **2004**, *16*, 4647. (b) Kietzke, T.; Hörhold, H.-H.; Neher, D. *Chem. Mater.* **2005**, *17*, 6532. (c) Manoj, A. G.; Alagiriswamy, A. A.; Narayan, K. S. *Appl. Phys. Lett.* **2003**, *94*, 4088.
(7) Ago, H.; Petritsch, K.; Shaffer, M. S. P.; Windle, A. H.; Friend, R. H. *Adv. Mater.* **1999**, *11*, 1281.
(8) Parker, I. D. *J. Appl. Phys.* **1994**, *75*, 1656.
(9) (a) Prosa, T. J.; Winokur, M. J.; Moulton, J.; Smith, P.; Heeger, A. J. *Macromolecules* **1992**, *25*, 4364. (b) Sirringhaus, H.; Brown, P. J.; Friend, R. H.; Nielsen, M. M.; Bechgaard, K.; Langeveld-Voss, B. M. W.; Spiering, A. J. H.; Janssen, R. A. J.; Meijer, E. W.; Herwig, P.; de Leeuw, D. M. *Nature* **1999**, *401*, 685. (c) Sirringhaus, H.; Tessler, N.; Friend, R. H. *Science* **1998**, *280*, 1741.

performance of the annealed device was significantly enhanced compared to the pristine one.[11] Transmission electron microscope (TEM) observation showed the enhancement of P3HT crystallinity and elongation of P3HT fibrillar crystals.

However, the influence of crystallinity enhancement and morphology change of the photoactive layer derived from a combination of dopants and conjugated polymers, consequently to enhance the performance of photovoltaic devices, has not yet been reported. Thus, this paper fills this research gap by explaining that SWNTs are found to originate for P3HT to form a uniform active layer with an interpenetrating network structure, which accounts for efficient photoinduced exciton generation and dissociation. Electron diffraction (ED) and TEM morphology confirm the enhancement of crystallinity and formation of microcrystals for P3HT on the sidewall of SWNTs, which contributes to pronounced enhancement of photovoltaic device performance.

Experimental Methods

Chemicals. P3HT used for this study was obtained from Aldrich. ($M_w = 87\,000$ g·mol^{-1}), and regioregularity is greater than 98.5% head-to-tail regiospecific conformation. SWNTs were obtained by the chemical vapor decomposition method. As-prepared products were treated by nitric acid and thermally oxidized to purify the SWNTs following a modified method described in ref 12. In short, 40 mg of as-prepared SWNTs were refluxed in 2.6 M nitric acid solution for 16 h; the sample was then separated by centrifuging and washed with copious deionized water. After drying the sample at about 100 °C, the nitric acid purified SWNTs were thermally oxidized in air at 450 °C for 4.5 h in a tube furnace. Nitric acid purified SWNTs having a large amount of amorphous carbon were chosen in this study for comparison to directly show the amount of hybridized carbon in the active layer given that amorphous carbon cannot be solubilized by conjugated polymer. TEM and scanning electron microscopy (SEM) were utilized to fully characterize the as-prepared and purified materials.

Device Fabrication. P3HT was dissolved in chloroform to prepare a solution with a concentration of 10 mg·mL^{-1}. SWNTs were dispersed in chloroform to obtain a suspension with the help of ultrasonication for 3 h. A series of solutions with desired concentrations were prepared by mixing designated amounts of the pristine P3HT solution and SWNTs suspension and then diluting to a final volume. Three SWNTs/P3HT composite solutions were prepared with the same P3HT concentration of 1 mg·mL^{-1} but with different amounts of SWNTs: (1) nitric acid purified SWNTs accounted for 1% of P3HT, (2) thermally oxidized SWNTs accounted for 1% of P3HT, and (3) thermally oxidized SWNTs accounted for 2% of P3HT. The composite solutions were then ultrasonicated for 5 min prior to spin coating.

Device fabrication was performed by spin coating with the designated composite solution on ITO-coated glass after necessary cleaning using acetone and a mixture of deionized water and ethanol (1:1). The spinning speed was set at 2000 rpm to control film thickness with about 100 nm obtained from AFM scanning. As shown in Figure 1, fabrication was finished by thermally evaporating aluminum top electrode film on the masked composite film surface to obtain several isolated solar cells.

Instrumentation. TEM images and ED patterns were obtained on a JEOL 100CX electron microscope operated at 100 KV. Purified SWNTs at each step were dispersed in chloroform, and the suspension was dropped on 400 mesh Cu grids with supporting carbon film. The

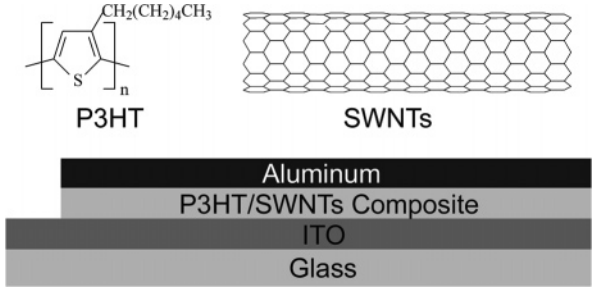

Figure 1. Chemical structure of P3HT and SWNTs, and schematic representation of a photovoltaic device.

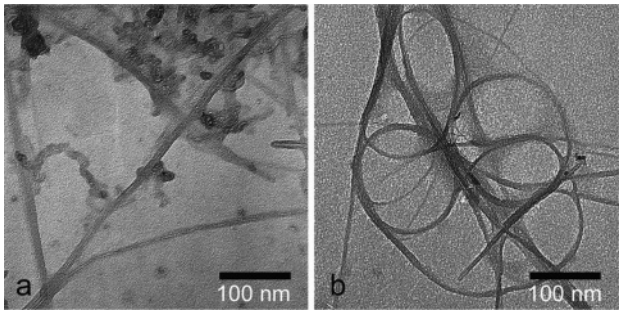

Figure 2. Morphology of (a) nitric acid purified SWNTs and (b) thermally oxidized SWNTs.

samples were observed by TEM after the solvent evaporated. A solution of purified SWNTs/P3HT composite in chloroform with designated concentrations was coated on a carbon film vacuum deposited on newly cleaved mica slides by spin coating at a spinning speed of 2000 rpm. Next, the sample film was transferred onto Cu grids by immersing the mica slides into deionized water to float the sample film onto the water surface and picking up the sample by naked Cu grids. Preparation was finished by vacuum deposition of a thin layer of carbon film on the polymer surface. SEM morphology observation and energy-dispersive X-ray spectroscopy (EDS) analyses were performed using a JEOL JSM 5400LV scanning microscope, operated at 20 KV.

Atomic force microscope (AFM) images were recorded on a PicoPlus 2500 manufactured by Molecular Imaging, Corp. A 10 μm scanner was used to control the scanning. The samples were prepared on glass slides with ITO coating with chloroform solution of purified SWNTs/P3HT composite having a designated concentration by spin coating at a spinning speed of 2000 rpm. A noncontact model was used to obtain the images.

Photovoltaic device testing was performed in an isolated black box to ensure standard calibration and reproducibility of results. $I-V$ characteristics were monitored using a Keithley 2400 source measurement unit. Using an AM1.5 global filter, white light illumination obtained from a 150 W Xenon lamp with a power of 33 mW·cm^{-2} was achieved by a Newport 69907 power supply.

Results and Discussion

The main impurities in the as-prepared SWNTs are cobalt catalyst and amorphous carbon, revealed by SEM morphology and EDS analyses. Nitric acid purification and thermal oxidization were performed to remove the catalyst and amorphous carbon, respectively. As shown in Figure 2, amorphous carbon continues to be an impurity in purified SWNTs using nitric acid, while the SWNTs surface becomes smooth after thermal oxidization. Carbon nanotubes have a tendency to bundle together due to van der Waals interaction so that individual tubes are hard to be seen without the aid of dispersant.

Solubilization and functionalization of SWNTs by polymers play a vital role in exploring and developing its application.

(10) Li, G.; Shrotriya, V.; Huang, J.; Yao, Y.; Moriarty, T.; Emery, K.; Yang, Y. *Nat. Mater.* **2005**, *4*, 864.
(11) Yang, X.; Loos, J.; Veenstra, S. C.; Verhees, W. J. H.; Wienk, M. M.; Kroon, J. M.; Michels, M. A. J.; Janssen, R. A. J. *Nano Lett.* **2005**, *5*, 579.
(12) Dillon, A. C.; Gennett, T.; Jones, K. M.; Alleman, J. L.; Parilla, P. A.; Heben, M. J. *Adv. Mater.* **1999**, *11*, 1354.

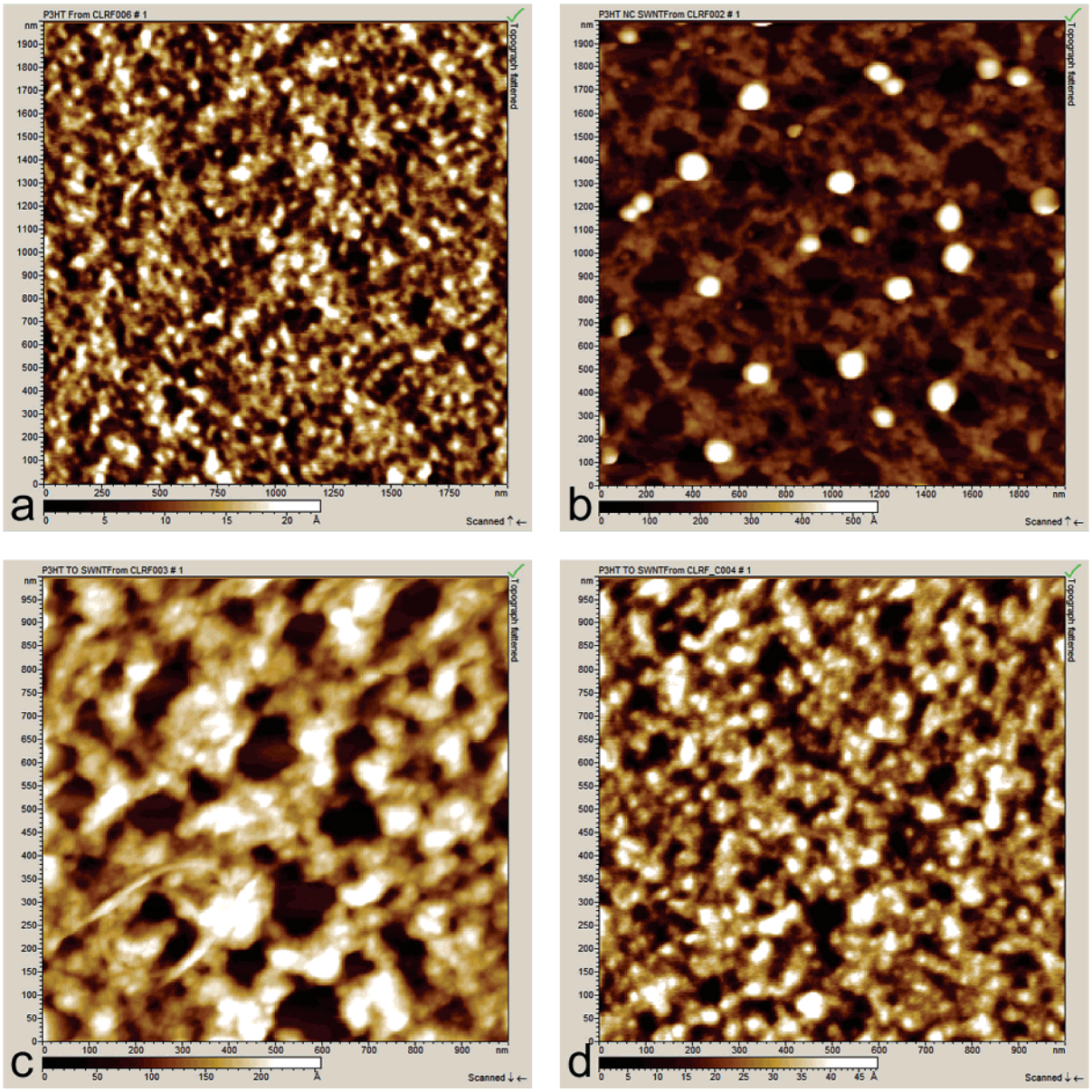

Figure 3. AFM topography of (a) pristine P3HT film with 2000 × 2000 nm^2 scanning range, (b) 1% nitric acid purified SWNTs/P3HT composite film with 2000 × 2000 nm^2 scanning range, (c) 1% thermally oxidized SWNTs/P3HT composite film with 1000 × 1000 nm^2 scanning range, and (d) 2% thermally oxidized SWNTs/P3HT composite film with 1000 × 1000 nm^2 scanning range.

Polymer wrapping, π-stacking, and selective interaction of the defective site of SWNTs to polymer were discovered to be interaction mechanisms between polymers and carbon nanotubes. Most of the research into polymer solubilization on SWNTs has focused on poly(phenylenevinylene) (PPV), poly(phenyleneethynylene) (PPE) having a benzene ring in the backbone,[13] poly(ethylene glycol)[14] and polymers having functional groups, especially atoms having a lone pair on the main chain.[15] However, few studies have reported on the solubilization or interaction between polythiophene and SWNTs, while this system is so important that polymer photovoltaic devices based on SWNTs/P3HT composite have frequently been reported.

The film morphology from chloroform solution of pristine P3HT and SWNTs/P3HT composites was observed by AFM at noncontact mode, as shown in Figure 3. A rough surface was formed by pristine P3HT (Figure 3a). Compared to pristine P3HT film, nitric acid purified SWNTs hybridized polymer film shows a much rougher surface. The round particles are derived from amorphous carbon because amorphous carbon cannot be solubilized by P3HT.[13b] Beneath the particles, SWNTs/P3HT composite forms a film with an interpenetrating network structure, which is critically beneficial for charge transportation. The interpenetrating network structure is further confirmed by TEM image, obtained with a relatively thinner thermally oxidized SWNTs/P3HT composite film (Figure 4). Figure 3c

(13) (a) Chen, J.; Liu, H.; Weimer, W. A.; Halls, M. D.; Waldeck, D. H.; Walker, G. C. *J. Am. Chem. Soc.* **2002**, *124*, 9034. (b) Dalton, A. B.; Stephan, C.; Coleman, J. N.; Mccarthy, B.; Ajayan, P. M.; Lefrant, S.; Bernier, P.; Blau, W. J.; Byrne, H. J. *J. Phys. Chem. B* **2000**, *104*, 10012. (c) Star, A.; Stddart, J. F.; Steuerman, D.; Diehl, M.; Boukai, A.; Wong, E. W.; Yang, X.; Chung, S.-W.; Choi, H.; Heath, J. R. *Angew. Chem., Int. Ed.* **2001**, *40*, 1721.

(14) Huang, W.; Fernando, S.; Allard, L. F.; Sun, Y.-P. *Nano Lett.* **2003**, *3*, 565.

(15) (a) Rouse, J. H. *Langmuir* **2005**, *21*, 1055. (b) O'Connell, M. J.; Boul, P.; Ericson, L. M.; Huffman, C.; Wang, Y.; Haroz, E.; Kuper, C.; Tour, J.; Ausman, K. D.; Smalley, R. E. *Chem. Phys. Lett.* **2001**, *342*, 265.

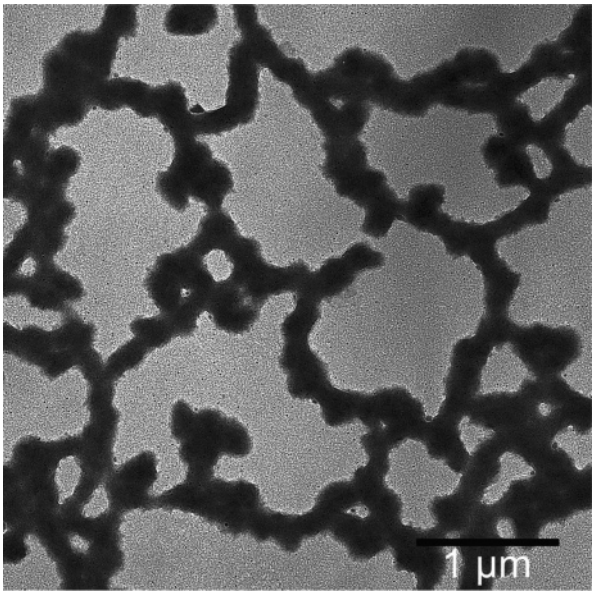

Figure 4. Interpenetrating network structure of SWNTs/P3HT composite film.

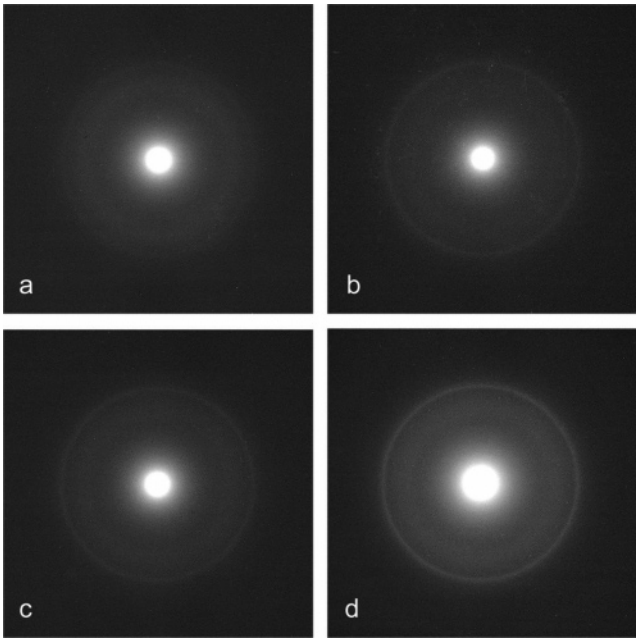

Figure 5. ED pattern of P3HT from (a) pristine P3HT, (b) 1% nitric acid purified SWNTs/P3HT composite, (c) 1% thermally oxidized SWNTs/P3HT composite, and (d) 2% thermally oxidized SWNTs/P3HT composite.

shows the AFM topography of thermally oxidized SWNTs/P3HT composite film. Compared to nitric acid purified SWNTs/P3HT composite film, amorphous carbon particles disappeared in the thermally oxidized SWNTs/P3HT composite film. In both of these cases (Figure 3b and 3c) hybridized carbon accounts for the same percentage in the composites, which means that the same amount of SWNTs in Figure 3c as that of amorphous carbon and SWNTs in Figure 3b dispersed uniformly in the composite film. Obviously, homogeneous dispersion of SWNTs in P3HT matrix is due to the solubilization effect of P3HTs to carbon nanotubes. A small bundle of carbon nanotubes is detected at the bottom left of the image in Figure 3c. Actually, SWNTs bundle was not easy to find while AFM scanning was performed. The image here purposely shows the existence of SWNTs in P3HT matrix. Thermally oxidized SWNTs/P3HT composite (with 2% SWNTs) displays a more uniform and consecutive film (Figure 3d) compared to the composites with a lower content of SWNTs. Obviously, higher carbon nanotube content will result in a denser distribution of small carbon nanotube bundles, even individual carbon nanotubes. A dense and uniform distribution of single carbon nanotubes constructs the framework of the composite film and further forms a consecutive composite film.

A TEM image is a two-dimensional projection of a three-dimensional structure in a thin film which loses morphology information in the direction normal to the film. Although Figure 4 merely gives a two-dimensional interpenetrating morphology, a three-dimensional interpenetrating structure actually exists considering the homogeneous distribution of SWNTs in P3HT matrix. The resultant interpenetrating network structure composed of P3HT microcrystals and small bundles of, even individual, carbon nanotubes provides a continuous tunnel in the entire active film for efficient electron and hole transportation. On the other hand, a homogeneous distribution of carbon nanotubes in P3HT matrix ensures achievement of maximum interface between SWNTs and P3HT. The interface of carbon nanotubes and polymer is the site to generate excitons upon light exposure. Therefore, effective solubilization of P3HT on SWNTs and homogeneous distribution of SWNTs in P3HT matrix guarantee efficient utilization of absorbed light to generate excitons.

From the solubilization mechanism of conjugated polymer on carbon nanotubes, π-stacking between them is the origination of the interaction. Therefore, π-stacking inevitably results in local molecular orientation in a nanoscale dimension along the wall of carbon nanotubes. The local molecular orientation is beneficial to quick crystallization of polymer from its solution as the solvent evaporates. Selected area ED method was used to characterize the crystallinity of P3HT in its SWNTs/P3HT composite as shown in Figure 5. The outer diffraction ring corresponds to a distance of 0.39 nm. This ring is attributed to (020) planes of P3HT crystals in which $\pi-\pi$ stacking of P3HT backbone is located. A diffraction arc or ring with the same *d* spacing was reported in previous work for ED patterns of P3HT whiskers.[11,16] The typical ED pattern shows the 020 diffraction ring becoming more intense with increases of the absolute content of SWNTs in P3HT, which confirms the inducing effect of carbon nanotubes on P3HT crystallization. Interestingly, the performance of a photovoltaic device is strongly dependent on the fabrication processing and condition. Thermally annealing the active layer to increase polymer crystallinity is usually used to improve the device efficiency for polymer photovoltaic devices. Microcrystalline structure is usually thought as an efficient intermedium for interchain transport of charge carriers. P3HT whiskers increase in length by over 50% upon thermal treatment for the PCBM/P3HT system; consequently, device efficiency was raised remarkably.[11] In our experiments SWNTs are utilized to raise the crystallinity of P3HT, and at the same time, SWNTs serve as electron acceptors and electron transport tunnel, efficiently increasing the exciton dissociation and charge transport. These results point to an important characteristic of the SWNTs/P3HT system. Effective solubilization of P3HT on carbon nanotubes ensures a homogeneous distribution of

(16) Ihn, K. J.; Moulton, J.; Smith, P. *J. Polym. Sci., Part B: Polym. Phys.* **1993**, *31*, 735.

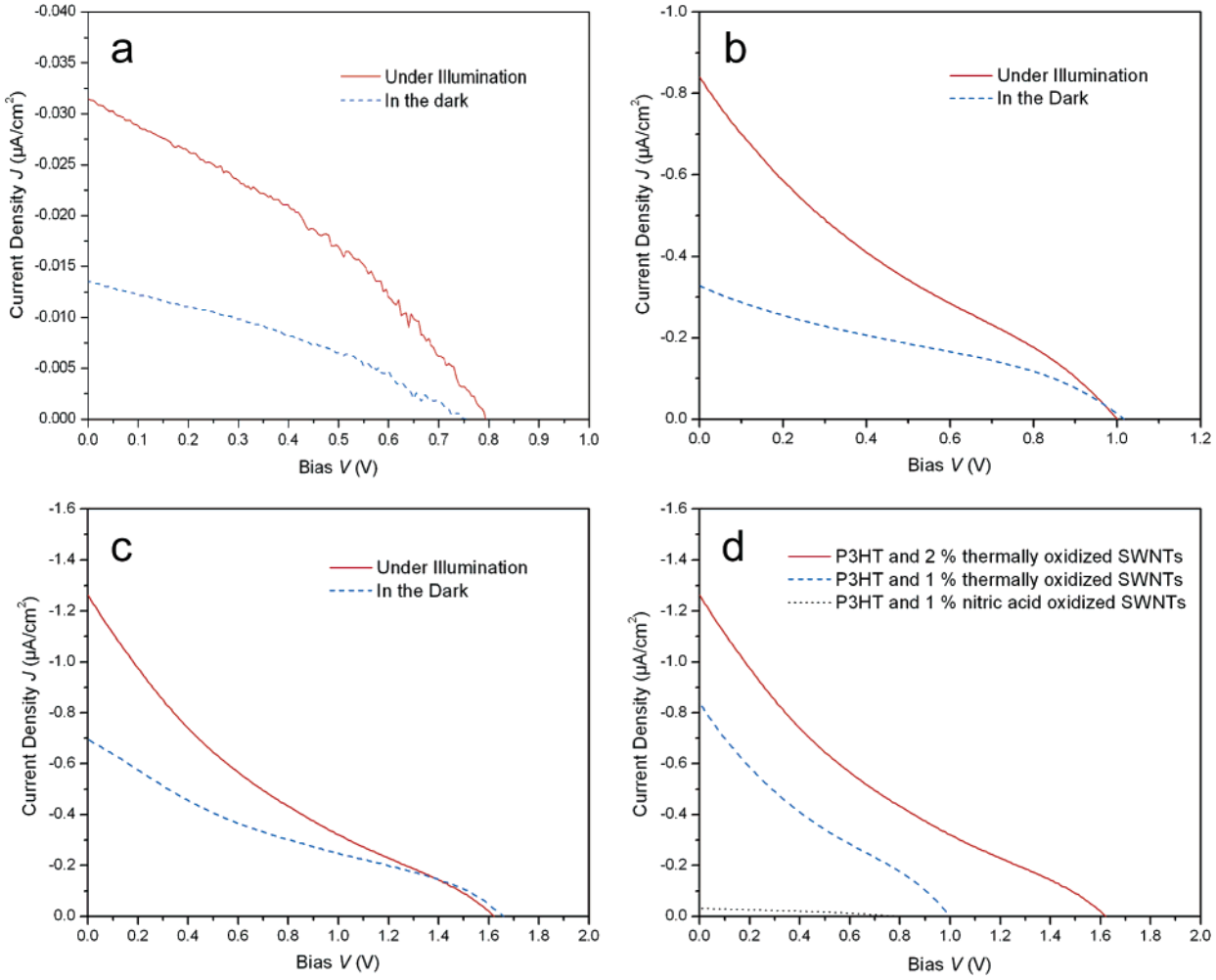

Figure 6. Performance of devices fabricated from SWNTs/P3HT composite with (a) 1% content of nitric acid purified SWNTs, (b) 1% content of thermally oxidized SWNTs, and (c) 2% content of thermally oxidized SWNTs, and (d) a comparison of performance of above devices under illumination.

SWNTs in SWNTs/P3HT composite. Higher electron affinity of SWNTs and their inducing effect to obtain a higher crystallinity of P3HT active layer are shown to be beneficial to exciton dissociation and charge carrier transport.

Figure 6 shows the current density−voltage ($I-V$ curve) characteristics of photovoltaic devices fabricated from SWNTs/P3HT composite with various content of carbon nanotubes. Compared to the device from composite with 1% thermally oxidized SWNTs (Figure 6b), the device from composite with 1% nitric acid purified SWNTs (Figure 6a) displays a relatively low short-circuit current density (I_{SC}). This is because the existence of amorphous carbon in nitric acid purified SWNTs (Figures 2a and 3b) cannot be dispersed homogeneously in the P3HT matrix nor obtain a big amount of efficient interface in SWNTs/P3HT composite to trigger exciton generation and dissociation. Increasing the hybridized content of thermally oxidized SWNTs in the SWNTs/P3HT composite efficiently enhanced the I_{SC} (Figure 6c). From the morphology and structure research described above, a relatively higher content of thermally oxidized carbon nanotubes produces uniform active film with interpenetrating network structure and enhances the crystallinity, which accounts for the remarkable increase of I_{SC}.

Figure 6d exhibits a comparison of $I-V$ features of photovoltaic devices fabricated from SWNTs/P3HT composite with different carbon nanotubes content. (The $I-V$ curve obtained in a relatively wider sweeping range is available in the Supporting Information.) Except for elevation of I_{SC} with increasing hybridized SWNTs in P3HT, the open-circuit voltage (V_{OC}) also shows a tendency to increase. A high V_{OC} of the photovoltaic device for the SWNTs/P3HT system has always been the focus of discussion since the birth of SWNTs/P3HT photovoltaic devices. Obviously, the traditional metal−insulator−metal model proposed by Parker for single-layer light-emitting diodes[8] cannot explain the occurrence of V_{OC} in this system because the experimental result is much higher than the calculated one, $V_{OC} = 0.4$ V from $\Phi_{ITO} = 4.7$ eV and $\Phi_{Al} = 4.3$ eV. This model requires that the active layer should have a negligible amount of intrinsic charge carriers and hence be regarded as an absolute insulator, for example, photovoltaic devices based on pure P3OT systems.[17] However, the active layer formed by SWNTs/P3HT composite in this work should not be viewed as an insulator because of metallic and semiconducting carbon nanotubes in it. The Fermi energy pinning mechanism was first proposed to be applied to the polymer/fullerene system[18] and then introduced to the devices based on SWNTs/P3OT composite.[4b] Ohmic-like behavior between SWNTs and negative electrode contact is a vital assumption to apply this mechanism. In this case, the upper limit of V_{OC} can be

(17) Kymakis, E.; Amaratunga, G. A. J. *Appl. Phys. Lett.* **2002**, *80*, 112.
(18) L. J. Brillson, *Surf. Sci. Rep.* **1982**, *2*, 123.

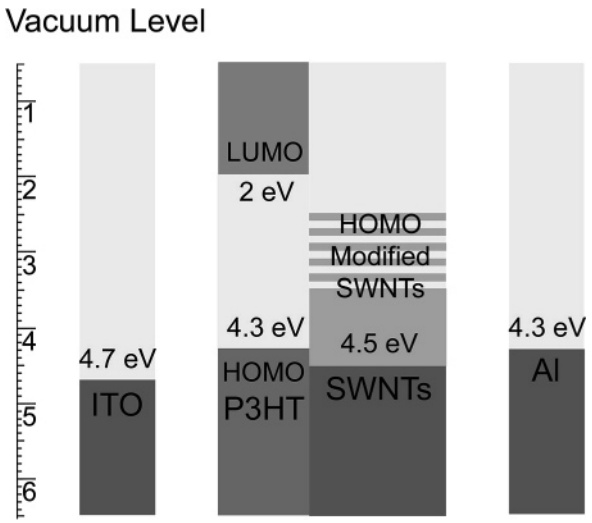

Figure 7. Potential-energy diagram of the SWNTs/P3HT system relative to vacuum level.

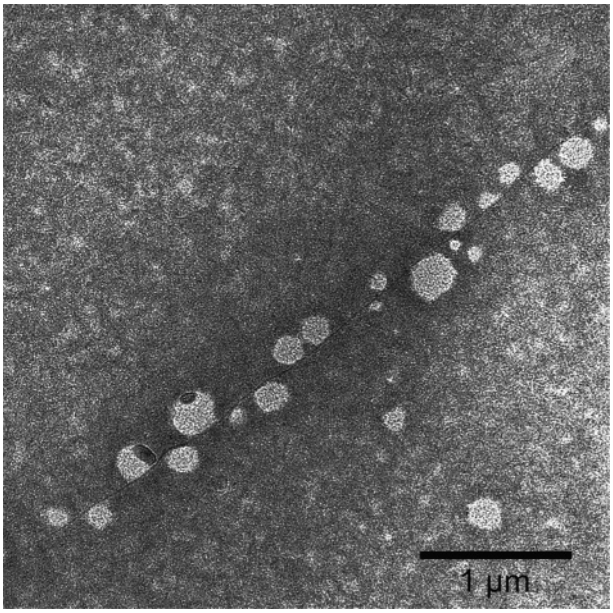

Figure 8. TEM morphology of P3HT microcrystals attached on the sidewall of SWNTs.

determined by the difference of carbon nanotubes work function and polymer HOMO level. Even so, the Fermi energy pinning mechanism still failed to address the high V_{OC}, as high as 1.6 V, especially when the HOMO level for P3HT (4.3 eV)[19] in our studies is lower than that of P3OT (5.25 eV).[4b]

A change of work function of SWNTs was investigated by intercalation of alkali metal (K, Rb, Cs).[20] Interestingly, it was found that the work function decreased dramatically upon alkali-metal intercalation. The electronic state near the Fermi level is significantly modified, and consequently, metallic and semiconducting tube bundles become indistinguishable. Intuitively, reduction of the work function can be understood by charge transfer from metal to carbon nanotubes, which shifts the Fermi level of the conduction band toward the vacuum.[20a] Transplanting this concept to the SWNTs/P3HT system, the Fermi level of carbon nanotubes might be influenced by attachment of polythiophene to their sidewall, further reducing the work function as shown in Figure 7. The zebra crossing represents the possible level range of HOMO for P3HT-modified SWNTs.

It is well known that defects, including dislocations, sp^3-hybridized carbon, and the presence of pentagons and heptagons, distribute on the sidewall or at the caps of carbon nanotubes. Among them, pentagonal defects in the lattice cause charge localization in the lattice structure. Sulfurs in the thiophene ring on the polymer chain are electron rich due to the electron pair on the sulfur atom. Therefore, strong interaction exists between thiophene segments on the polymer chain and pentagon defects on the carbon nanotubes. A similar binding was reported between an alkoxy phenylene segment on poly(*m*-phenylene-vinylene-co-2,5-dioctoxy-*p*-phenylenevinylene) (PmPV) chain and a pentagonal defect on carbon nanotubes.[21] Figure 8 shows that P3HT microcrystals originate from the sidewall of SWNTs. The bright appearances are P3HT crystals because of their relative density, and a similar result for P3HT whiskers was observed in previous studies.[11] P3HT microcrystals with an approximate diameter of 500 nm align along a filament of nanotubes like a string of pearls, and the SWNTs bundle is so thin that it is just barely detected. Such thin SWNTs bundle is hard to observe without solubilization of P3HT, confirming the interaction between SWNTs and P3HT and further supporting the strong electron transfer from polymer chain to carbon nanotubes. Interaction sites of P3HT to carbon nanotubes densely distribute on the sidewall of SWNTs as deduced from the dense distribution of microcrystals of P3HT affixed to SWNTs, which infers the extent of electron transferring from P3HT to carbon nanotubes. As shown in Figure 7, the Fermi level is shifted toward to the vacuum level after SWNTs is modified with P3HT. Reduction of the work function of P3HT-modified SWNTs accounts for the high V_{OC} of the photovoltaic device based on the SWNTs/P3HT system. From Figure 6d, V_{OC} increases with the content of SWNTs. This is probably caused by reduction of contact resistance between carbon nanotubes, and metal electrodes and nanotubes with increase of SWNT content.

Conclusions

We have demonstrated the interaction between SWNTs and P3HT by observation of morphology change of polymer film formed by SWNTs/P3HT composite and formation of P3HT micro-
crystals on the sidewall of carbon nanotubes. SWNTs disperse in the active layer homogeneously, which results in a large interface for photoinduced exciton formation and exciton dissociation. In addition, SWNT serves as an additive reagent to elevate the crystallinity for P3HT based on local order of polymer chain along the sidewall of carbon nanotube, which accounts for the performance improvement of photovoltaic devices. Work-function-modulated reduction of the HOMO level for SWNTs based on electron transfer from sulfurs on the polymer chain to SWNTs explains the occurrence of high open-circuit voltage.

Acknowledgment. We thank Dr. John Andersland of Western Kentucky University for his assistance with TEM images. This

(19) Mikalo, R. P.; Schmei*β*er, D. *Synth. Met.* **2002**, *127*, 273.
(20) (a) Zhao, J.; Han, J.; Lu, J. P. *Phys. Rev. B* **2002**, *65*, 193401. (b) Suzuki, S.; Bower, C.; Matanabe, Y.; Zhou, O. *Appl. Phys. Lett.* **2000**, *76*, 4007.
(21) Mccarthy, B.; Coleman, J. N.; Curran, S. A.; Dalton, A. B.; Davey, A. P.; Konya, Z.; Fonseca, A.; Nagy, J. B.; Blau, W. J. *J. Mater. Sci. Lett.* **2000**, *19*, 2239.

work is partially supported by the Junior Faculty Scholarship at Western Kentucky University through the Office of Sponsored Programs, by the U.S. National Science Foundation under contract #0520789, and by KY NSF EPSCoR REG Program under contract #260501.

Supporting Information Available: $I-V$ curve obtained in a relatively wider sweeping range. This material is available free of charge via the Internet at http://pubs.acs.org.

JA065035Z